

Biophysical Journal, Volume 111

Supplemental Information

Mechanism of Axonal Contractility in Embryonic *Drosophila* Motor Neurons In Vivo

Alireza Tofangchi, Anthony Fan, and M. Taher A. Saif

List of Figures

S1	Log-linear plot of contraction dynamics of six randomly chosen axons. Sets of experimental data are colored in solid lines. Corresponding best linear fits are graphed in dotted lines.	3
S2	Cartoon Schematics. (A) Graphical representation of various notation used. (B) Procedures of control experiments. (C) Procedures of pharmaceutical experiments. . .	4
S3	Axon contraction inhibited by ML-7 (A) and Y-27632 (B). Effect of ML-7 (C) and Y-27632 (D) at approximately 67% & 33% of the concentration reported in the main text. N=6 in all cases. All error bars in standard deviation. Note that ML-7 at the applied concentration may lead to the inhibition of PKA, PKC, and other pathways.	5
S4	DIC, anti- α -tubulin, and neuronal-membrane-bound-GFP composite images with (A) and without (B) drug. Expanded images of microtubules morphology with (C) and without (D, reduced image gain by one-eighth due to saturation) drug. (E-J) Images obtained with a brief extraction step before fixation. Anti- α -tubulin and neuronal-membrane-bound-GFP composite images with (E, G, & I) and without (F, H, & J) drug. The composite images are separated into the two channels indicating the presence of polymerized microtubules (G & H) and neuronal membrane (I & J). Same imaging conditions applied unless otherwise noted.	6
S5	Glial cells visualizations, through staining (A-B) and crossing (C-F), show high degree of glial ensheathment of uncleaned axon, and minimal ensheathment along the axon shaft of cleaned axon. (A) DIC and anti-repo composite image of preparation. Cleaned axon on the left. (B) Anti-repo channel of A. (C & E) Phase and glial-membrane-bound-GFP composite images at 2 different focal planes. Cleaned axon on the right. (D & F) Glial-membrane-bound-GFP channel of C & E respectively. . .	7

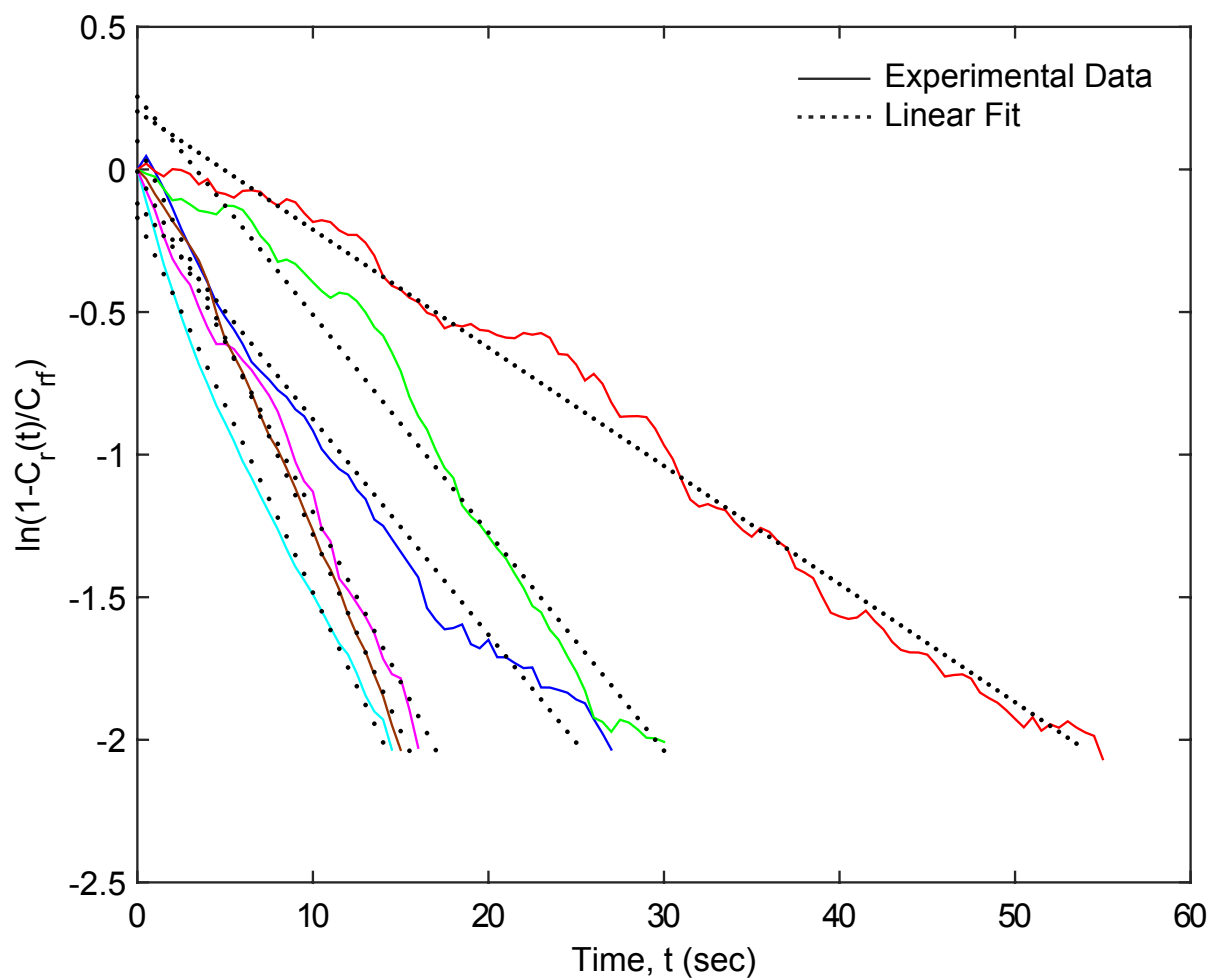


Figure S1: Log-linear plot of contraction dynamics of six randomly chosen axons. Sets of experimental data are colored in solid lines. Corresponding best linear fits are graphed in dotted lines.

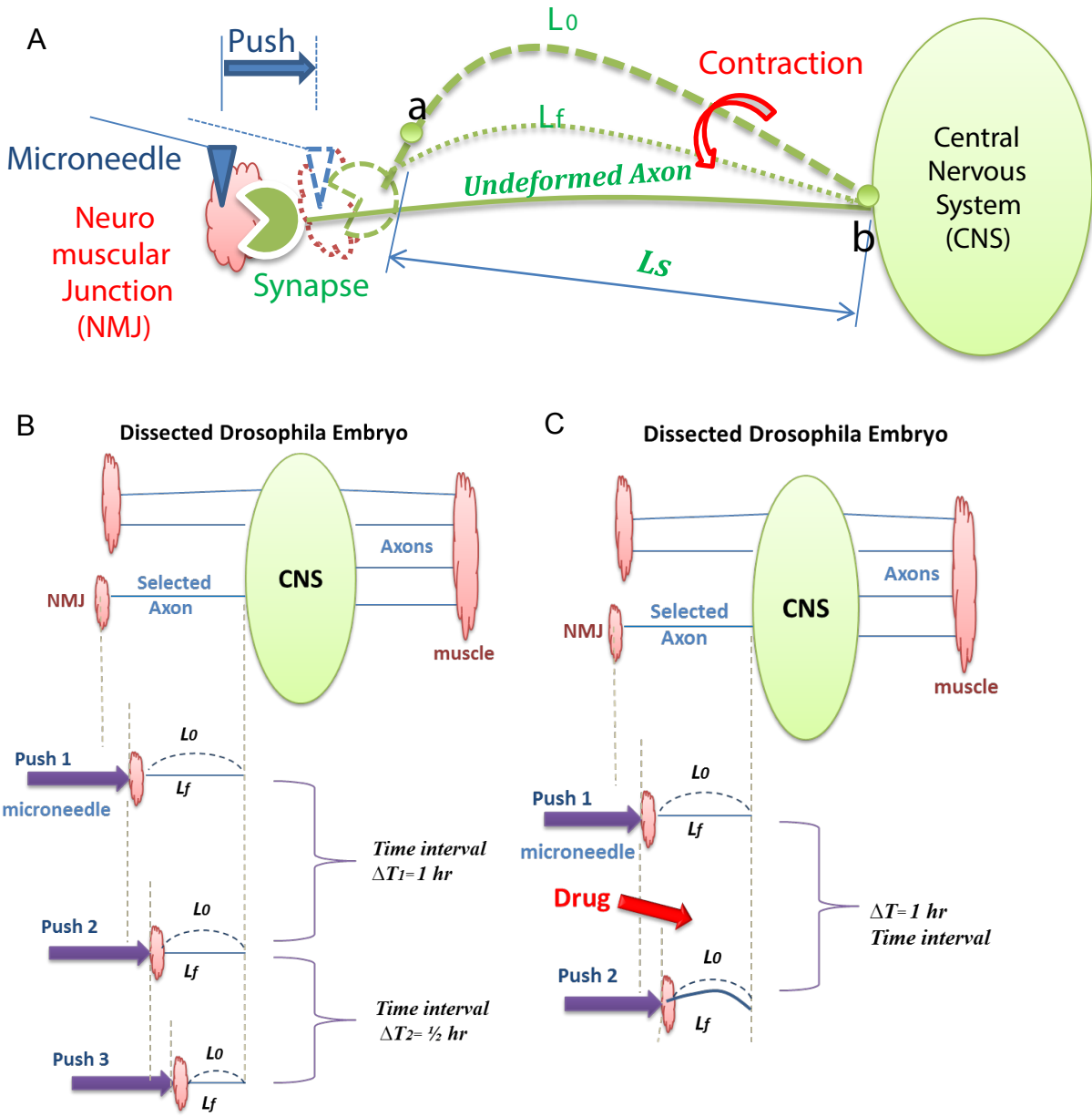


Figure S2: Cartoon Schematics. (A) Graphical representation of various notation used. (B) Procedures of control experiments. (C) Procedures of pharmaceutical experiments.

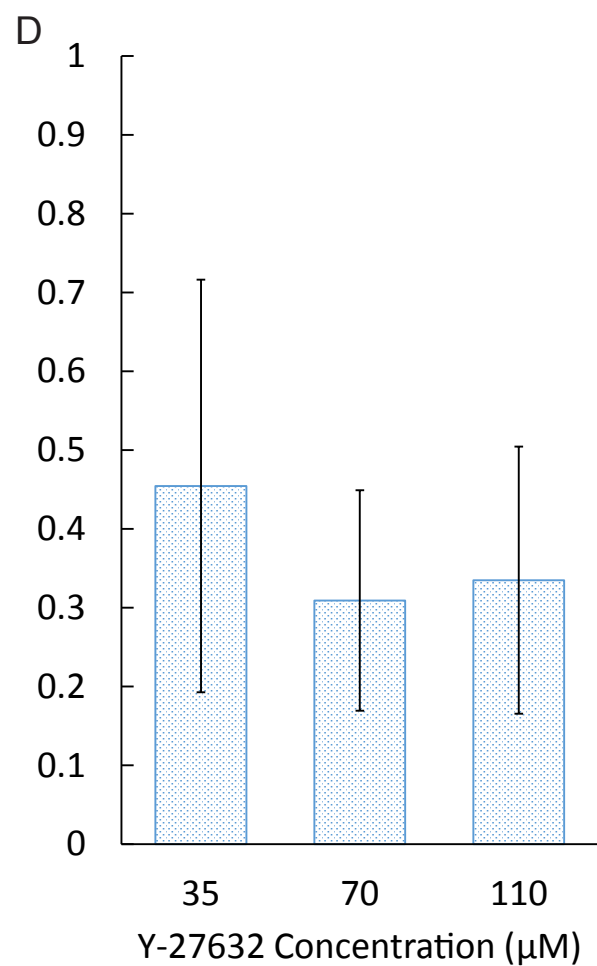
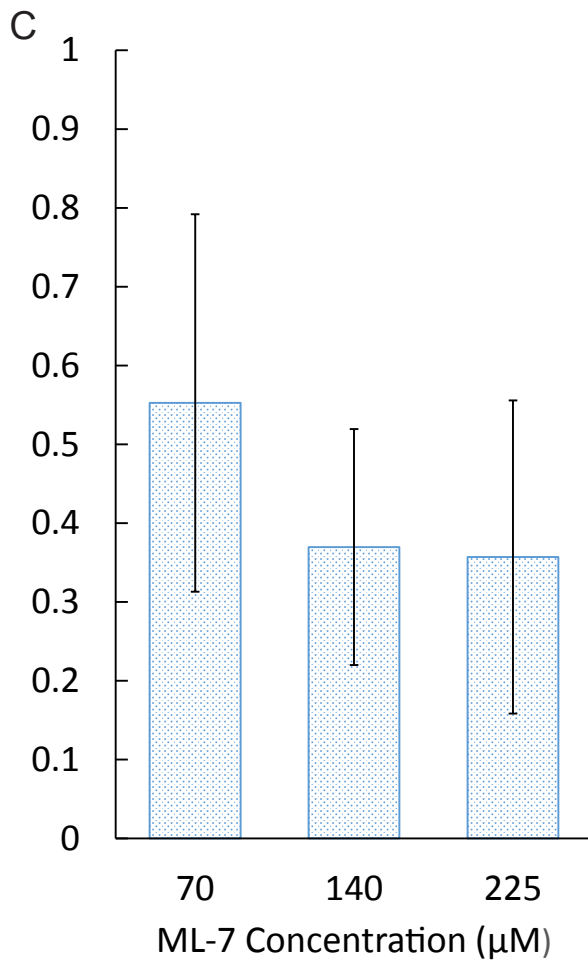
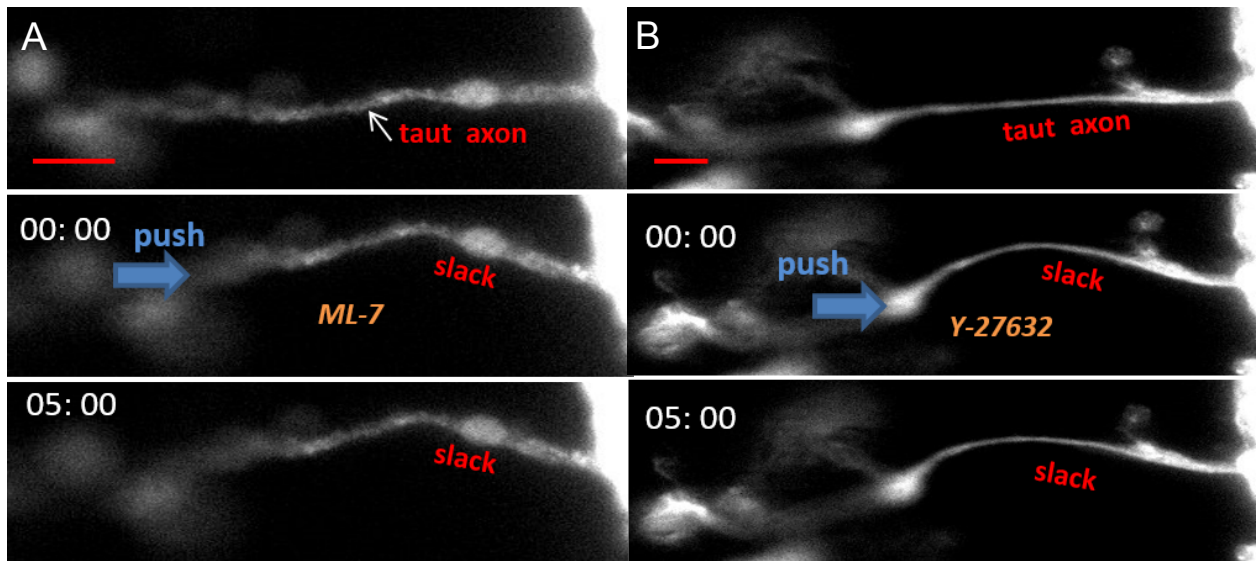


Figure S3: Axon contraction inhibited by ML-7 (A) and Y-27632 (B). Effect of ML-7 (C) and Y-27632 (D) at approximately 67% & 33% of the concentration reported in the main text. N=6 in all cases. All error bars in standard deviation. Note that ML-7 at the applied concentration may lead to the inhibition of PKA, PKC, and other pathways.

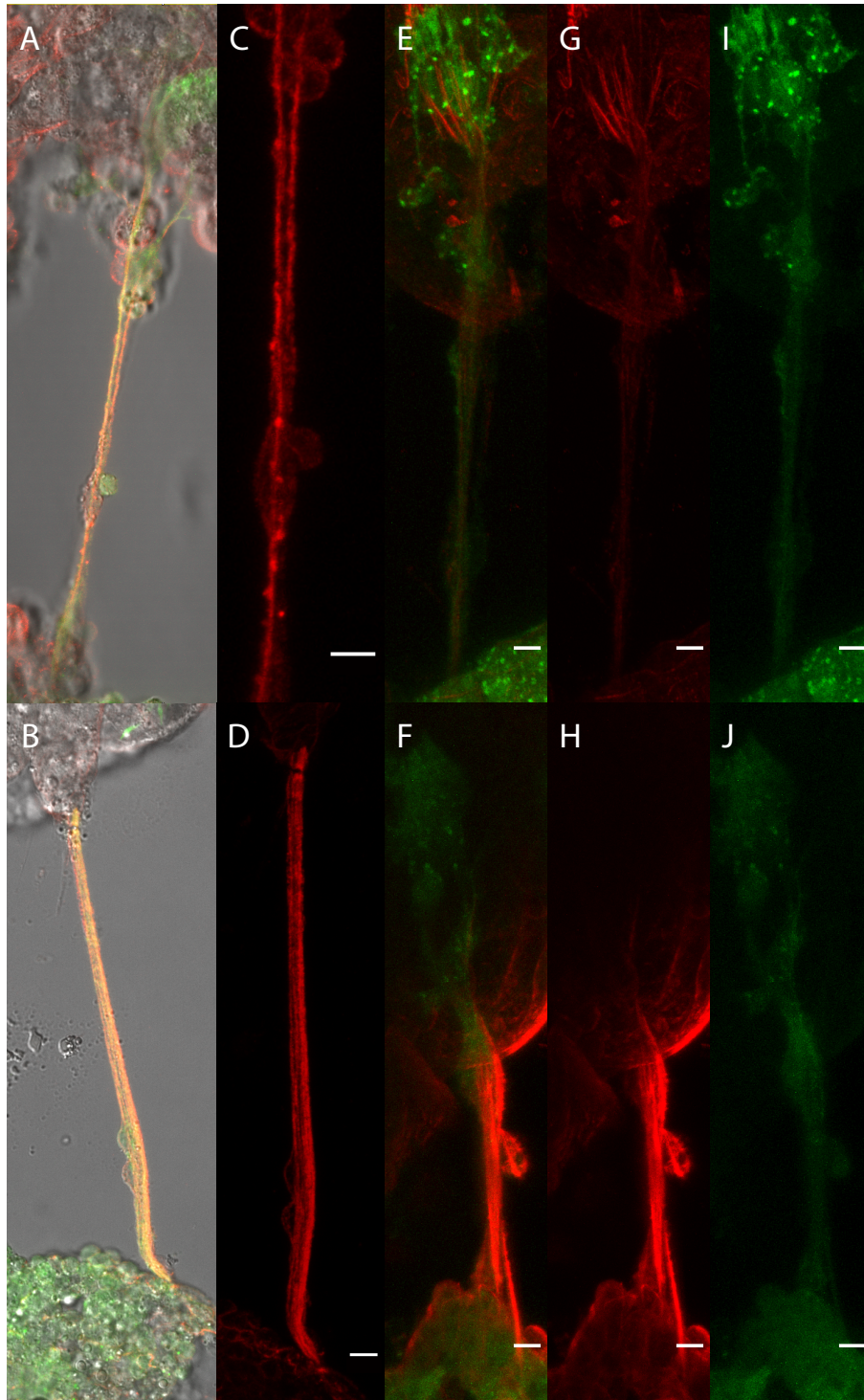


Figure S4: DIC, anti- α -tubulin, and neuronal-membrane-bound-GFP composite images with (A) and without (B) drug. Expanded images of microtubules morphology with (C) and without (D, reduced image gain by one-eighth due to saturation) drug. (E-J) Images obtained with a brief extraction step before fixation. Anti- α -tubulin and neuronal-membrane-bound-GFP composite images with (E, G, & I) and without (F, H, & J) drug. The composite images are separated into the two channels indicating the presence of polymerized microtubules (G & H) and neuronal membrane (I & J). Same imaging conditions applied unless otherwise noted.

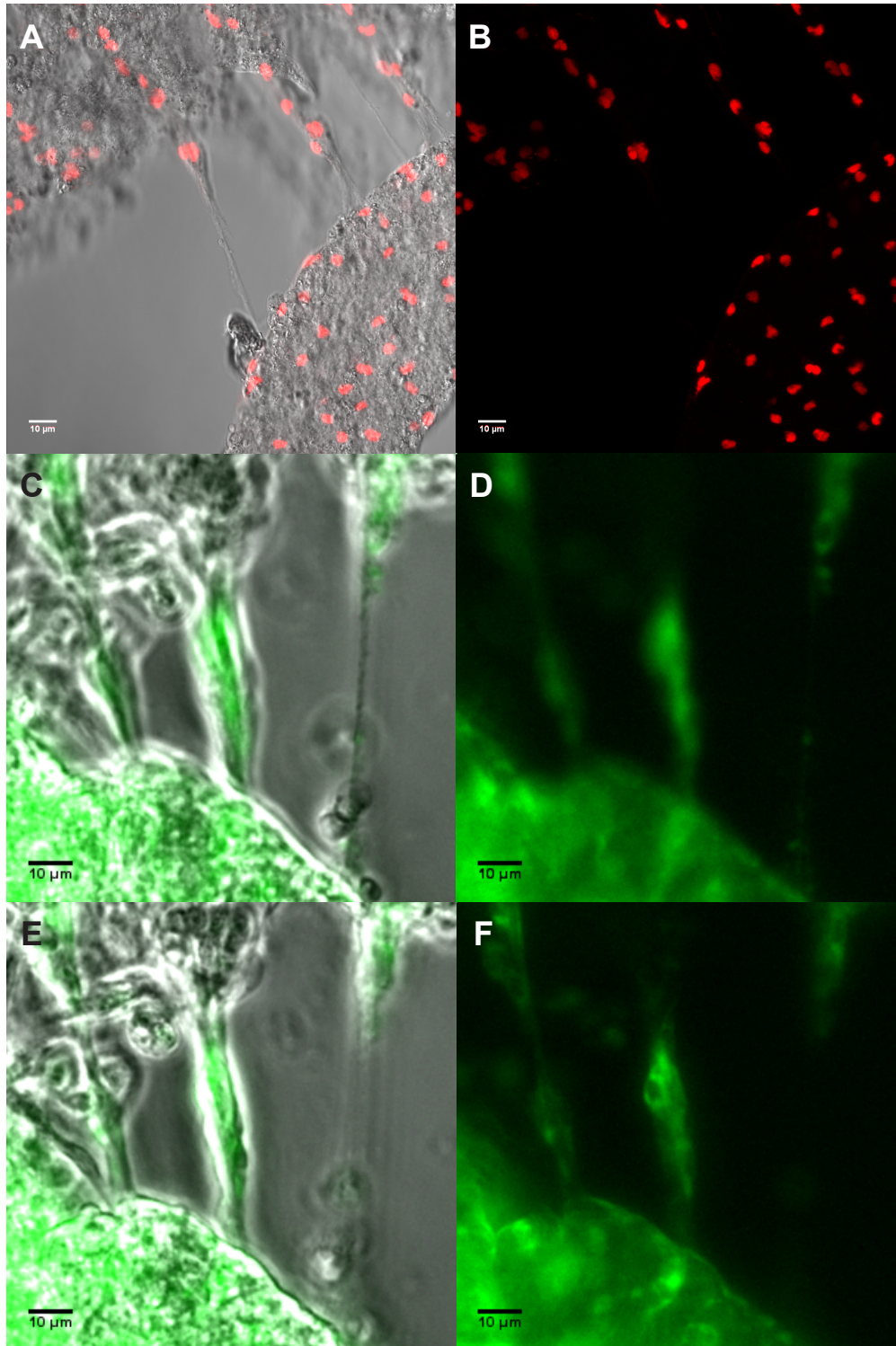


Figure S5: Glial cells visualizations, through staining (A-B) and crossing (C-F), show high degree of glial ensheathment of uncleaned axon, and minimal ensheathment along the axon shaft of cleaned axon. (A) DIC and anti-repo composite image of preparation. Cleaned axon on the left. (B) Anti-repo channel of A. (C & E) Phase and glial-membrane-bound-GFP composite images at 2 different focal planes. Cleaned axon on the right. (D & F) Glial-membrane-bound-GFP channel of C & E respectively.